doi: 10.34312/jgeosrev.v5i1.17333 ejurnal.ung.ac.id/index.php/jgeosrev

Vol. 5, No. 1, January 2023: 51-62

Jambura Geoscience Review

p-ISSN 2623-0682 | e-ISSN 2656-0380

Department of Earth Science and Technology, Universitas Negeri Gorontalo

Contribution of Resistivity Properties in Estimating Hydraulic Conductivity in Ciremai Volcanic Deposits

Deden Zaenudin Mutaqin [1], Hendarmawan[1], Agus Didit Haryanto[1], Undang Mardiana[1], Febriwan Mohammad[1]

[1] *Faculty of Geological Engineering, Padjadjaran University, Jatinangor, 45363, West Java, Indonesia*

ARTICLE INFO

Article history:
Received: 6 December 2022
Accepted: 9 January 2023
Published: 25 January 2023

Keywords:
Hydraulic Conductivity; Resistivity; Pourus Aquifer; Volcano

Corresponding author:
Deden Zaenudin Mutaqin
Email: deden13005@mail.unpad.ac.id

ABSTRACT

The hydraulic parameters of porous media, such as porosity (φ) and hydraulic conductivity (K), are the most important factors for planning and managing water exploitation from aquifers. This study aims to estimate the hydraulic conductivity parameters using the geoelectric method on volcanic deposits on the northern slope of Mount Ciremai. For this purpose, four data types were used to estimate K and φ, including lithological profiles, water table, groundwater quality, pumping test data, and vertical electrical sounding (VES). Based on Archie's law and Kozeny's equation, we get the alpha (α) values and cementation factor (m) from which the median values of $\alpha = 1.01$ and $m = 1.36$ represent the studied aquifer. The porosity (φ) of the aquifer varies from 0.097 to 0.187 with an average of 0.141 and is spatially related to the hydraulic conductivity (kgm), which varies from 4.97 × 10-6 to 6.75 × 10-5 m/s after the application of Kozeny's equation. The hydraulic conductivity (Kp) calculated from the pumping tests varies from 9.07×10^{-6} to 1.06×10^{-4} m/s and is strongly correlated ($r = 0.87$). Furthermore, a relation between resistivity and hydraulic conductivity was established for the studied aquifer to estimate these parameters in sites lacking data.

How to cite: Mutaqin, D. Z., Hendarmawan, H., Haryanto, A. D., Mardiana, U., & Mohammad, F. (2023). Contribution of Resistivity Properties in Estimating Hydraulic Conductivity in Ciremai Volcanic Deposits. *Jambura Geoscience Review, 5*(1), 51-62. doi:https://doi.org/10.34312/jgeosrev.v5i1.17333

1. INTRODUCTION

The hydraulic parameters of porous media, such as porosity (φ) and hydraulic conductivity (K), are the most important factors for planning and managing water exploitation from aquifers (Amiri et al., 2022). Hydrogeological methods such as pumping tests have been widely used to estimate the hydraulic parameters of aquifers because they provide a high level of reliability. In addition, this method is not economical, time-consuming, and requires large data sets to estimate the aquifer's hydraulic parameters (Soupios et al., 2007; Tizro et al., 2010).

An alternative method for hydrogeological field procedures is hydrogeophysics, one of which is resistivity (Alfadli & Natasia, 2017; Darisma et al., 2020; Kazakis et al., 2016). Resistivity properties and aquifer hydraulic characteristics can be correlated because there is a relationship between transmissivity and transverse resistance (Ungemach, Mostaghimi, & Duprat, 1969). Since then, a large number of studies have been carried out on the estimation of aquifer parameters using geoelectrical equations. Kazakis et al. (2016) estimated the porosity and hydraulic conductivity using Archie (1942) and Kozeny equation. The porosity of a porous aquifer can be estimated using the cementation factor (m) and the parameter alpha (α) (Archie, 1942). Cementation factor parameters (m) and alpha (α) play a key role in the estimation of hydrological parameters, whereas the m factor cannot be quantified directly from any laboratory test (Kwader, 1985). However, when other factors, such as water resistivity, are known, the value of m can be obtained by trial and error (Kwader, 1985). Additionally, the cementation factor (m) can be calculated using graphical methods of varying porosity and saturation resistivity measurements for a given formation (MacCary, 1978). Sattar et al. (2016) estimated the aquifer parameters using VES measurements in Northwest Bangladesh. Hasan et al. (2018) delineated the groundwater potential zones using the surface geophysical method in the Mian Channu area of Pakistan. The above studies established mathematical relations to estimate hydraulic parameters from surface resistivity measurements. These studies suggested that estimating hydraulic parameters using surface resistivity approaches is feasible. However, such relationships depend on specific areas and may have limited applications in other areas. In addition, the determination of aquifer resistivity is based on the range of resistivity correlated with geological conditions. So any range of resistivity values from ves is considered an aquifer layer (Ezema et al., 2020).

Estimating hydraulic conductivity in volcanic aquifers is challenging because this system contains great complexity, uncertainty, and ambiguity in applying geophysical methods, especially resistivity. Therefore, it is mandatory to adopt an integrated approach using multiple sources of data and information to find a reliable solution. From the results of this study, it is hoped that the geoelectric method can replace the pumping test method commonly used to find the value of the hydraulic conductivity coefficient of the subsurface in volcanic deposits.

2. METHOD

2.1. Data Sets

The research area is located on the northern slope of the Ciremai volcano, Rajagaluh District, Majalengka Regency, West Java, about 20 km from the city of Majalengka and 80 km from the city of Bandung with an elevation from 98 to 220 masl. The geology of the research area is composed of undifferentiated young volcanic products and undifferentiated old volcanic products. The undifferentiated young volcanic products are scattered in almost all research areas and consist of breccia, andesite, basaltic lava, tuffaceous sand, and lapilli from Mount Ciremai. The undifferentiated old volcanic products consist of volcanic breccia, lahar deposits, and andesitic and basaltic lava (Djuri, 1995). The volcanic aquifer system in the study area has heterogeneous aquifer characters with high productivity in soil weathering pore media and new rock fracture media (IWACO – WASECO, 1989). A more detailed study was conducted by Irawan et al. (2009). They found three hydrogeological systems have been pictured based on the 3 clusters consecutively. The 1st system is developed in a shallow, unconfined aquifer with high bicarbonate meteoric water domination. The 2nd system is predominated by mixing processes between groundwater in the unconfined aquifer and hot groundwater from deeper aquifers. The 3rd system is primarily dominated by groundwater flow from the deep formation

This study used four data types to estimate K and φ, including lithological profiles, water table, groundwater quality, pumping test data, and vertical electrical sounding (VES). The equipment in this research is geological field survey equipment (compass, hammer, loupe, GPS), hydrogeological field survey equipment (multiparameter Hanna, groundwater level measuring instrument, water pump, tool write for the pumping test), geoelectrical field survey equipment (Electrode, Power supply, Cable, Hammer, handheld GPS, HT communication device, and Martiel Geophysics Resistivity Meter Type MG1260).

Lithological profiles were carried out on exposed rocks. The main thing is to search the river flow because there is a greater chance of uncovering rocks. The object of observation in this study is rock. The aspects observed are descriptive, including physical properties, structure, and grain size. The lithological profiles of the area are based on data recorded at 48 outcrops (Figure 1). According to these data, two lithofacies, including volcanic breccia and tuff, were identified. Measurement of groundwater level and electric conductivity in thirty-nine (39) dug wells, and its spatial distribution is shown in Figure 1.

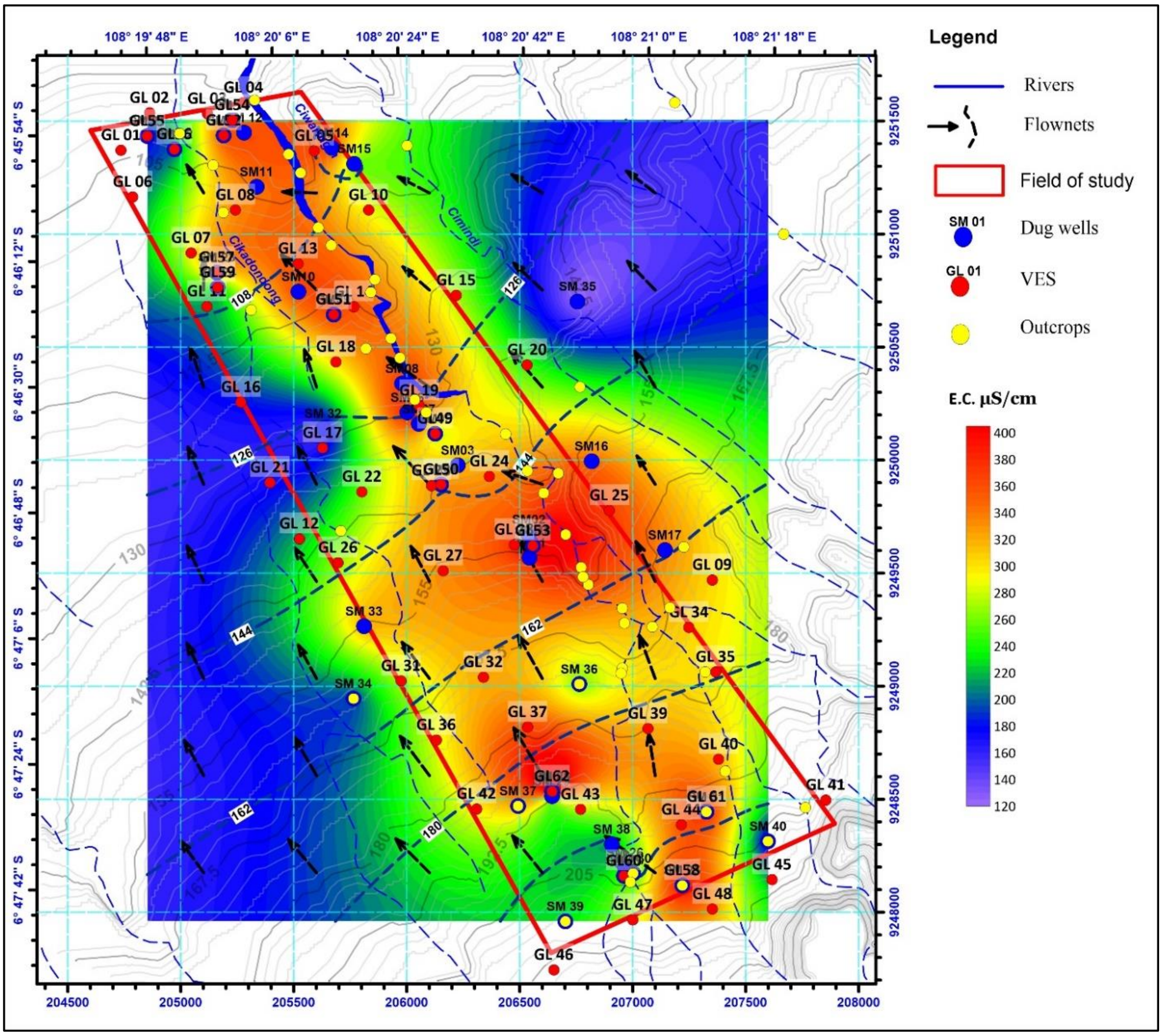

Figure 1. Measurement points and electrical conductivity of the groundwater

A total of seventeen pumping test data were used in this study. Self-carried out the pumping test data used in this study. The pumping test data were evaluated using the constant pumping rate discharge method. The pumping rates were within 0.3 l/ sec – 0.9 l/ sec, and the pumping time varies from 2 – 4 hrs. The principle of a pumping test involves applying stress to an aquifer by extracting groundwater from a pumping well and measuring the aquifer response to that stress by monitoring drawdown as a function of time. The obtained pumping test data were incorporated into an appropriate well flow equation (i.e., Theis recovery formula, Jacobs-Cooper drawdown-time formula) to determine in-situ aquifer characteristics. The transmissivity of the aquifers from pumping tests was determined by the Theis recovery method and Jacob Cooper's drawdown method (Cooper & Jacob, 1946; Theis, 1935).

Data from forty-four (44) vertical geoelectrical soundings (VES) were used for this research. The VES measurements were performed with a maximum half-current electrode separation of 200 m (the Schlumberger electrodes array was used). Vertical Electrical Sounding (VES) is a geoelectric method through the measurement of sounding to obtain information on the layer below the ground surface using the Schlumberger configuration. Equation Factor geometry Schlumberger is:

$$K_{fg} = \pi\left(\frac{L^2 - l^2}{2l}\right) \quad (1)$$

where ℓ point sounding spacing with the potential electrode and *L* point sounding spacing with the current electrode (Telford et al., 1990). Measurements were taken with a Naniura instrument, and

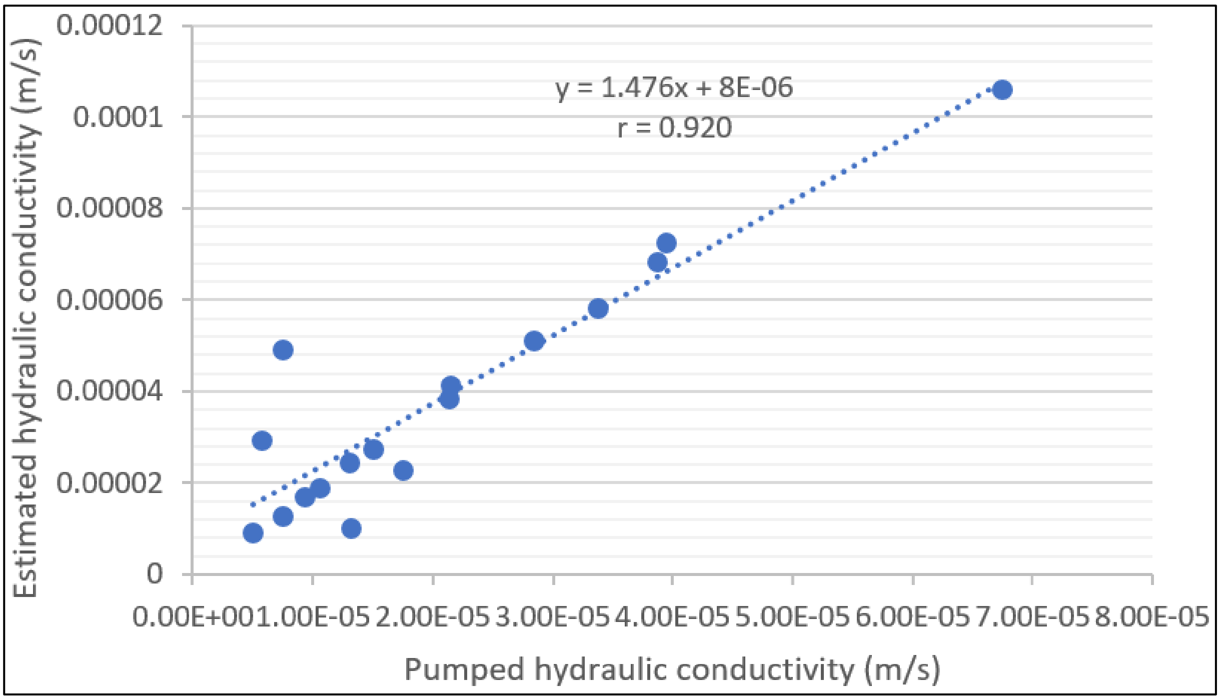

Figure 2. Correlation between K estimated from the median values of α and m and K obtained from pumping tests.

the inversion was performed using PROGRESS software; the RMS values varied between 3% and 7%. The sites of the geoelectrical soundings were close to existing pumping tests and lithological profiles and selected to cover the highest possible area of the porous aquifer. All VES data were used to estimate the aquifers' resistivity, whereas forty-four (44) data points were used to estimate the aquifer's hydraulic parameters.

2.2. Estimation of Hydraulic Parameters

2.2.1. Determination of cementation factor and alpha parameter

The cementation factor parameters (m) and alpha (α) are coefficients from Archie's law (Archie, 1942; Archie, 1950) that have been modified by Winsauer et al. (1952) and are expressed by the following Eq. 2:

$$\rho = \alpha . \rho w . \varphi^{-m} \qquad (2)$$

where ρ: bulk resistivity (Ohm-m), α: alpha parameter is the coefficient of void space in rock formations (coefficient of saturation), ρ_w: groundwater resistivity (Ohm-m), φ: porosity, m: factor cementation.

The values of α and m are very important to calculate the porosity using Eq.(2). In this study, the values of α and m were calculated from the hydraulic conductivity (k) recorded in the pumping test analysis, by applying the Cooper-Jacob method to be representative for the porous aquifer on the north slope of Ciremai volcano. The pumping test was carried out with a controlled pump rate for 3 hours, and the water level response was measured.

Firstly, porosity was calculated using (Kozeny, 1953) Eq.3 (Domenico & Schwartz, 1998) for the 17 sites in which the hydraulic conductivity (k) was known:

$$k = (\delta\omega g/\mu).(d\verb|^|2/180).[\varphi\verb|^|3 - \varphi)\verb|^|2\,] \qquad (3)$$

where δω is the water density (1000 kg/m^3), g is the acceleration due to gravity (9.81 m/s^2), and μ the dynamic viscosity of water (0.0014 kg/m s) (Fetter, 1994). According to the dug well's core samples, the average grain size (d) ranges between 0.00021 to 0.00049 m. In terms of porosity, Eq. 3 can be written as follows:

$$\delta\omega . g . d^2 . \varphi^3 - 180 . k . \mu . \varphi^2 + 360 . k . \mu . \varphi - 180 . k . \mu = 0 \qquad (4)$$

$$Pumping\ test \rightarrow \begin{pmatrix} Kp_1 \\ \vdots \\ Kp_6 \end{pmatrix} \rightarrow k = \left(\frac{\delta \omega g}{\mu}\right) \cdot \left(\frac{d^2}{180}\right) \cdot \left[\frac{\varphi^3}{(1-\varphi)^2}\right] \rightarrow \begin{pmatrix} \varphi_1 \\ \vdots \\ \varphi_6 \end{pmatrix} \rightarrow \begin{pmatrix} ln\alpha = lnFi_1 + m.\, ln\varphi_1 \\ \vdots \\ ln\alpha = lnFi_6 + m.\, ln\varphi_1 \end{pmatrix} \rightarrow$$

$$[\alpha_{modus} \quad m_{modus}] \rightarrow \begin{bmatrix} ln\alpha_{modus} = lnFi_1 + mmod.\, ln\acute{\varphi}_1 \\ \vdots \\ ln\alpha_{modus} = lnFi_6 + mmod.\, ln\acute{\varphi}_6 \end{bmatrix} \rightarrow \begin{bmatrix} \acute{\varphi}1 \\ \vdots \\ \acute{\varphi}6 \end{bmatrix} \rightarrow \begin{bmatrix} \acute{k}1 \\ \vdots \\ \acute{k}6 \end{bmatrix}$$

$$\begin{bmatrix} \alpha_1 & m_1 \\ \vdots & \vdots \\ \vdots & \vdots \\ \vdots & \vdots \\ \alpha_{15} & m_{15} \end{bmatrix} \rightarrow [\alpha_{mean} \quad m_{mean}] \rightarrow \begin{bmatrix} ln\alpha_{mean} = lnFi_1 + mmea.\, ln\acute{\varphi}_1 \\ \vdots \\ ln\alpha_{mean} = lnFi_6 + mmea.\, ln\acute{\varphi}_6 \end{bmatrix} \rightarrow \begin{bmatrix} \acute{\varphi}1 \\ \vdots \\ \acute{\varphi}6 \end{bmatrix} \rightarrow \begin{bmatrix} \acute{k}1 \\ \vdots \\ \acute{k}6 \end{bmatrix} \rightarrow$$

$$[\alpha_{median} \quad m_{median}] \rightarrow \begin{bmatrix} ln\alpha_{median} = lnFi_1 + mmed.\, ln\acute{\varphi}_1 \\ \vdots \\ ln\alpha_{median} = lnFi_6 + mmed.\, ln\acute{\varphi}_6 \end{bmatrix} \rightarrow \begin{bmatrix} \acute{\varphi}1 \\ \vdots \\ \acute{\varphi}6 \end{bmatrix} \rightarrow \begin{bmatrix} \acute{k}1 \\ \vdots \\ \acute{k}6 \end{bmatrix}$$

$$Correlation\ with\ [kp1 \ldots kp6] \rightarrow \begin{bmatrix} \alpha \\ m \end{bmatrix}$$

Figure 3. Flowchart of the process used to estimate the cementation factor (m) and alpha (α) parameter using excel software.

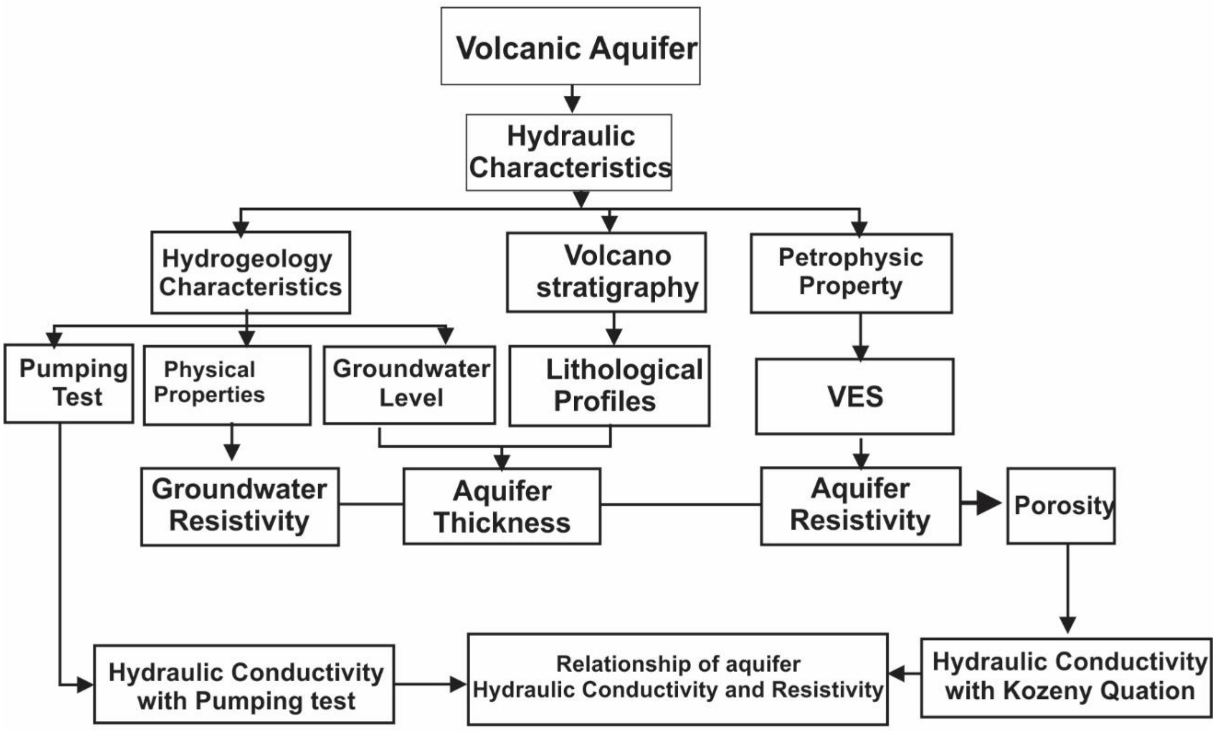

Figure 4. Flowchart showing the interconnection between the measured and estimated data of the studied aquifer.

The roots of this trinomial equation are two complex numbers, and a real number considered the only accepted value corresponds to the estimated porosity. The mean value of calculated porosity was 0.14, ranging from 0.097 to 0.18. In the next step, the calculated porosity values were used in Eq.2 (as described above), which was transformed to:

$$\ln\alpha = \ln Fi + m.\ln\varphi \tag{5}$$

Since the aquifer and groundwater resistivity values are known from hydrogeological mapping, 17 equations (one for each pumping test site) were formulated with two variables (α and m). The value of α and m were finally calculated from the solution of the pairs of the seventeen produced equations by pairs using Excel in which the values of Fi were known (Fi = ρ /ρw). A total of 136 α and m values were initially calculated (after removing negative and extreme values >3), and their mode, mean and median values were then estimated. The values of Fi originate from the resistivity of the aquifer and its groundwater in the same sites as the pumping test. These values were then used to estimate three sets of hydraulic conductivities (k) based on mode, average, and median values of α and m. The highest correlation (r = 0.920) was achieved when the median values were applied. Therefore, the values of α and m were chosen to be 1.01 and 1.36, respectively. This correlation is depicted in Figure 2, where kgm is the hydraulic conductivity estimated from the median values of α and m. A simplified flowchart of the proposed process is presented in Figure 3.

2.2.2. Determination of aquifer properties

Following the calculation of the α and m factors, The aquifer porosity was estimated for the remaining geoelectrical measurement sites using modified Archie's law (Archie, 1942; Archie, 1950) from Winsauer et al., (1952) Eq. 2 and its transformation Eq. 5 (Soupios et al., 2007).

$$\varphi = e^{\frac{1}{m}\ln(\alpha)+\frac{1}{m}\ln\left(\frac{1}{fi}\right)} \quad (6)$$

Then, the hydraulic conductivity is calculated using Eq. 3. Regression analysis of the aquifer resistivity and estimated hydraulic conductivity from the above procedure was carried out to establish the relationship between the two parameters in the studied aquifer. Figure 4 presents all the data used by the geoelectrical methods and the interconnection between the measured and estimated data of the studied aquifer.

3. RESULTS AND DISCUSSION

Field surveys were focused along the two main rivers to identify the lithological facies. Several lithostratigraphic logs were collected to define the lateral continuity of the geological formations. The study area is divided into two lithofacies: the tuff-lapilli tuff facies and tuff breccia-pyroclastic breccia intercalation with lapilli tuff facies (Figure 5). Tuff breccia-pyroclastic breccia intercalation with lapili tuff facies consist of tuff breccia, pyroclastic breccia and lapili tuff. These facies has the characteristics of poor sorting, massive-reverse bed structure, andesite rock components, and dominant lithic matrix composition. Based on the above characteristics, this facies is a product of lahar deposits (Figure 6). Lapilli tuff facies consists of medium-coarse tuff and lapilli tuff. These facies has the characteristics of well-moderately sorting, massive-graded bed structure, andesite rock components, and dominant lithic matrix composition. Based on the above characteristics, this facies is a product of pyroclastic flow deposits (Figure 7).

These facies outcrops are then correlated with resistivity data where each point is close to the other. The subsurface lithologies are interpreted on a local basis relating to the nature and characteristics of the rocks in that area (Gao et al., 2018). Several geoelectric points are adjacent to the outcrop, including ST 46 with GL 35 and ST 37 with GL 26 (Figure 8). Resistivity values in the study area range from 12 to 145 ohmmeters. Each lithofacies will later know the hydraulic conductivity value from the resistivity value. The tuff-lapilli facies has a resistivity range of fewer than 50 ohmmeters, and the tuff breccia-pyroclastic breccia intercalation with lapilli tuff facies has a resistivity range of more than 50 ohmmeters.

Based on the hydrogeological mapping, the study area shows the direction of groundwater flow from southeast to northwest or following the slopes (Ismawan et al., 2013), and electrical conductivity values range from 120 to 400 S/cm. The distribution of EC values is shown in Figure 1, where high EC values are in the main Ciwaringin river, while low EC values are in tributaries. Figure 9 shows the VES point used in determining hydraulic conductivity. This point is correlated with the water table of the dug well. The resistivity value at the dug well water table will determine the hydraulic conductivity.

After determining the most appropriate values of α and m (1.01 and 1.36), the aquifer's hydraulic parameters were calculated for the remaining seventeen locations using Archie's law and Kozeny's equation. Hydraulic conductivity (Kp) values computed from the pumping tests at the selected dug wells are given in Table 1. Afterward, empirical relations between the hydraulic parameters (hydraulic conductivity measured by pumping test) and the electrical parameters

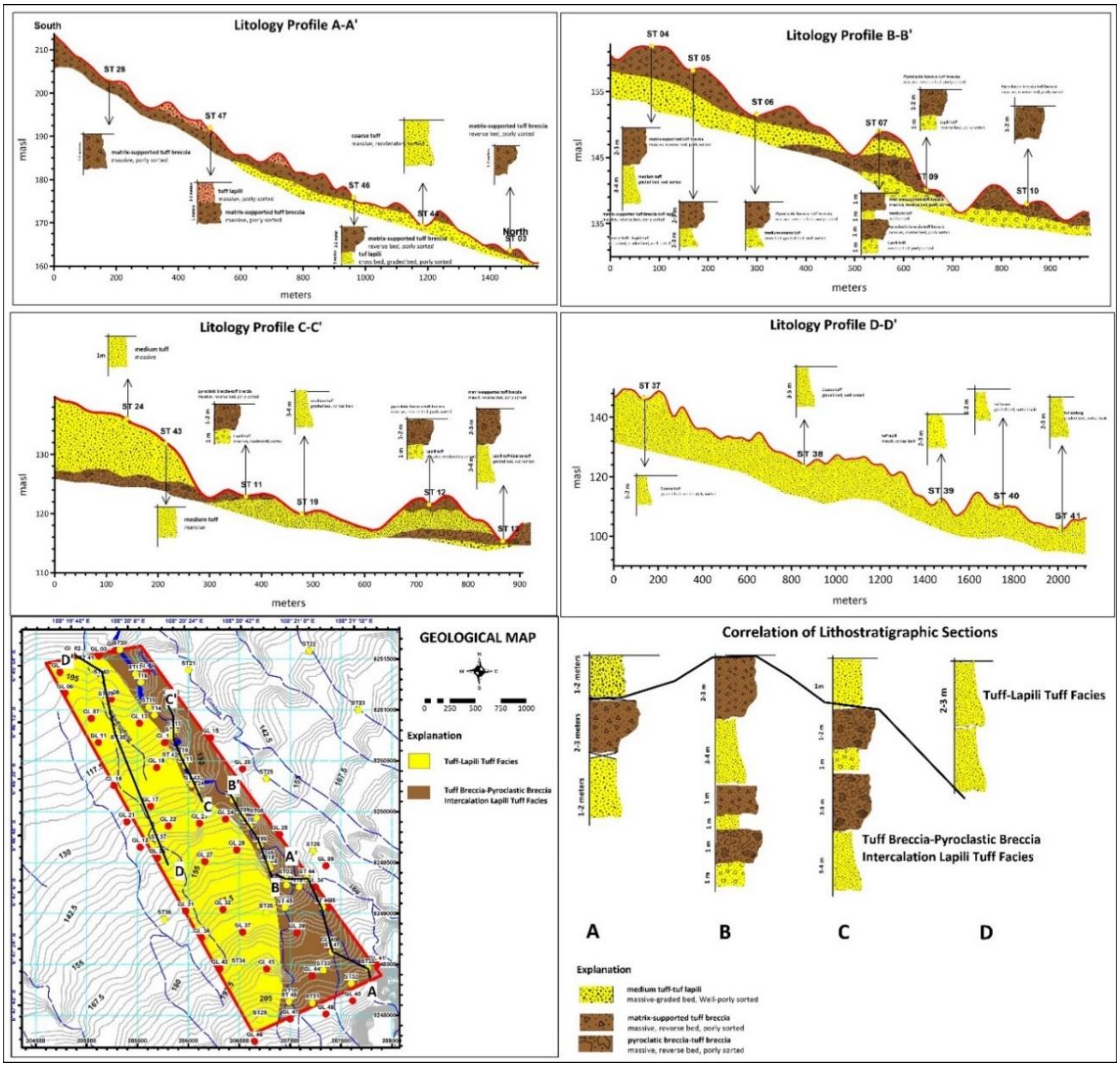

Figure 5. Correlation of simplified lithostratigraphic sections of the North slope of Ciremai Volcano.

Figure 6. Tuff breccia-pyroclastic breccia intercalation lapili tuff facies

(aquifer resistivity calculated from VES data) at the selected stations near the dug wells were established to estimate hydraulic conductivity (K) for all sounding.

The porosity (φ) of the aquifer varies from 0.097 to 0.187 with an average of 0.141 and is spatially related to the hydraulic conductivity (kgm), which varies from 4.97×10^{-6} to 6.75×10^{-5} m/s after the application of Kozeny's equation (Kozeny, 1953). The hydraulic conductivity (Kp) calculated from the pumping tests varies from 9.07×10^{-6} to 1.06×10^{-4} m/s and is strongly correlated ($r = 0.87$) with the respective kgm, as mentioned above. Regression analysis of the

Figure 7. Tuff - lapilli tuff facies.

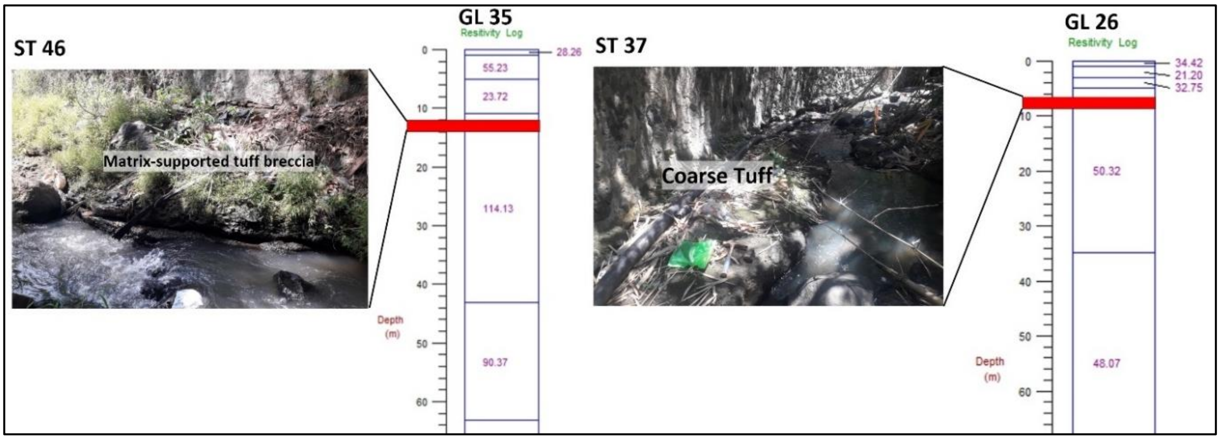

Figure 8. Correlation of resistivity values with outcrops.

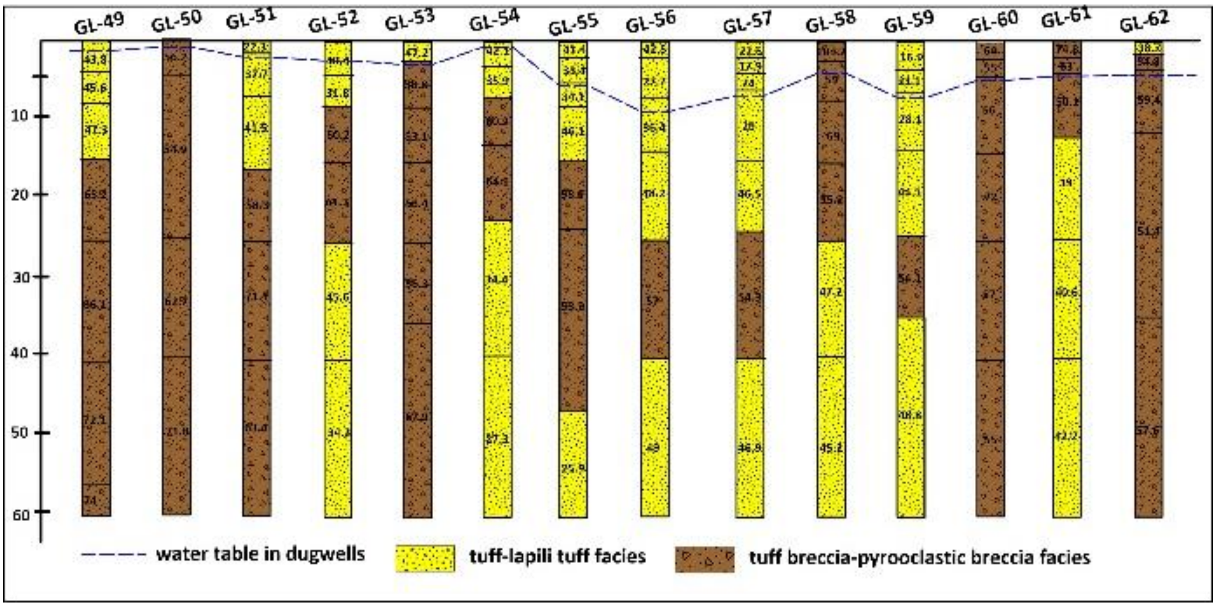

Figure 9. Comparison between the geoelectric and water table for selected fourteen stations in the study area.

aquifer's resistivity and estimated hydraulic conductivity (kes) (Figure 10) indicated the following relationship:

$$\text{kes} = 1.91 \times 10^{-4}.\, e^{-0.0492\rho} \tag{7}$$

The relationship between kgm and ρ can be combined with the relationship (8) between k estimated and k pumped (Figure 2) to rectify k regarding the k pumped provided from the pumping tests.

$$\text{kes} = 1.476\text{kp} + 7.762 \times 10^{-6} \tag{8}$$

Table 1. Resistivity and hydraulic parameter values following the application of geoelectrical methods.

VES	Well	Water table (m)	ρ (ohm.m)	ρw (ohm.m)	porosity	kgm (m/s)	kp (m/s)
GL49	SM 05	2.38	54	3.45	0.160	1.31E-05	2.45E-05
GL50	SM 04	1.4	56.2	3.33	0.125	1.5065E-05	0.0000274
GL51	SM 09	1.97	37.7	2.77	0.147	2.8485E-05	0.0000511
GL52	SM 13	1.94	40.4	3.03	0.143	2.1349E-05	0.0000384
GL53	SM 18	2.23	58.8	2.63	0.102	4.9769E-06	9.07E-06
GL54	SM 19	0.7	60.2	2.94	0.136	5.7209E-06	0.0000294
GL55	SM 21	6.15	34.1	3.33	0.187	6.7534E-05	0.000106
GL56	SM 22	9.12	36.4	3.33	0.179	3.3772E-05	0.0000582
GL57	SM 23	7.13	29	2.56	0.169	3.9503E-05	0.0000726
GL58	SM 25	4.6	59	2.50	0.097	1.0582E-05	0.0000189
GL59	SM 24	7.4	28.1	2.56	0.174	3.8719E-05	0.0000681
GL60	SM 27	3.54	56	4.00	0.147	1.3209E-05	0.0000101
	SM 26	4.7		4.17	0.153	1.7545E-05	0.0000228
	SM 30	5.1		4.17	0.151	2.1537E-05	0.0000412
GL62	SM 28	3.05	59.4	2.94	0.115	9.3683E-06	0.000017
	SM 29	0.78		2.94	0.114	7.5059E-06	0.0000128
GL 61	SM 31	5.05	74	2.63	0.108	7.4971E-06	0.0000492

$$\mathrm{kp} = \frac{1.91 \times 10^{-4}.\,e^{-0.0492\rho} - 7.762 \times 10^{-6}}{1.476} \tag{9}$$

This relationship (9) could be used to identify the spatial distribution of the hydraulic conductivity in the porous aquifer of the North slope Ciremai volcano in sites lacking pumping tests or wells by simply performing VES measurements and calculating the aquifer's resistivity.

Figure 11 compares the resistivity and hydraulic conductivity maps at 1m, 5m, and 20m depths. Figures 11a and 11b show resistivity maps with the same resistivity pattern at 1 m and 5 m depth with a resistivity value range of 13-143 ohm.m low resistivity values are shown in the northwest area, and high resistivity values are in the southeast area. When associated with the study area's

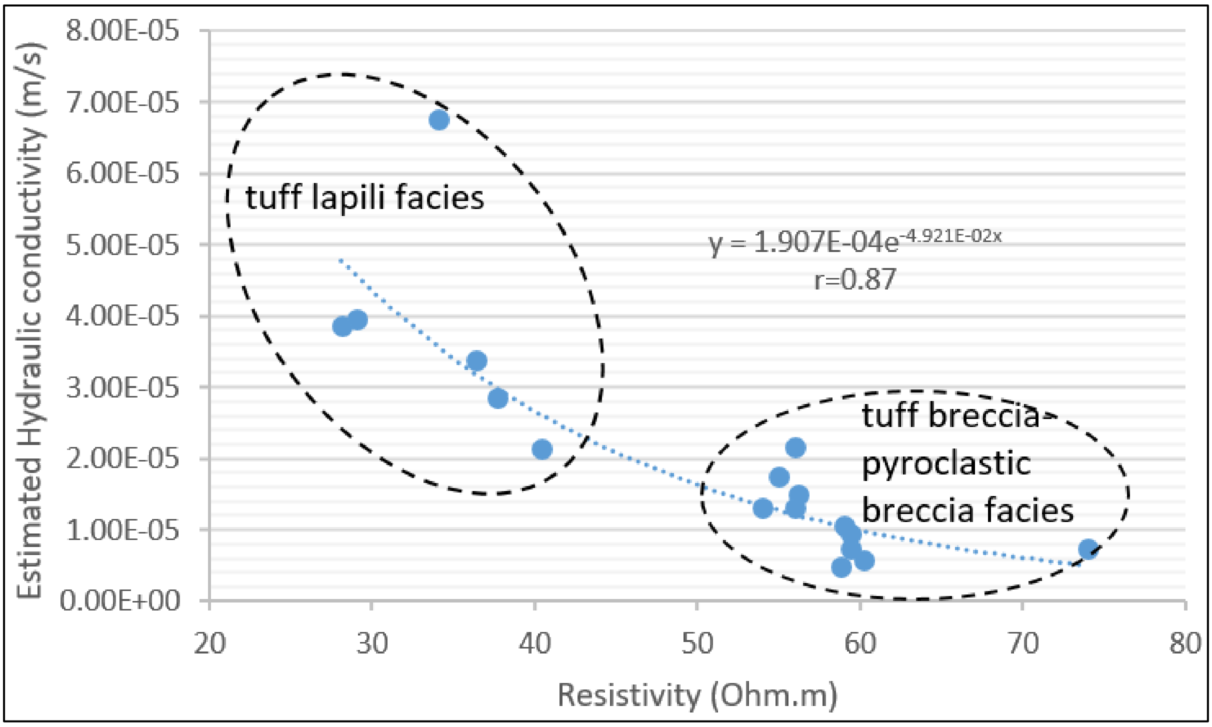

Figure 10. Relationship of aquifer hydraulic conductivity and resistivity

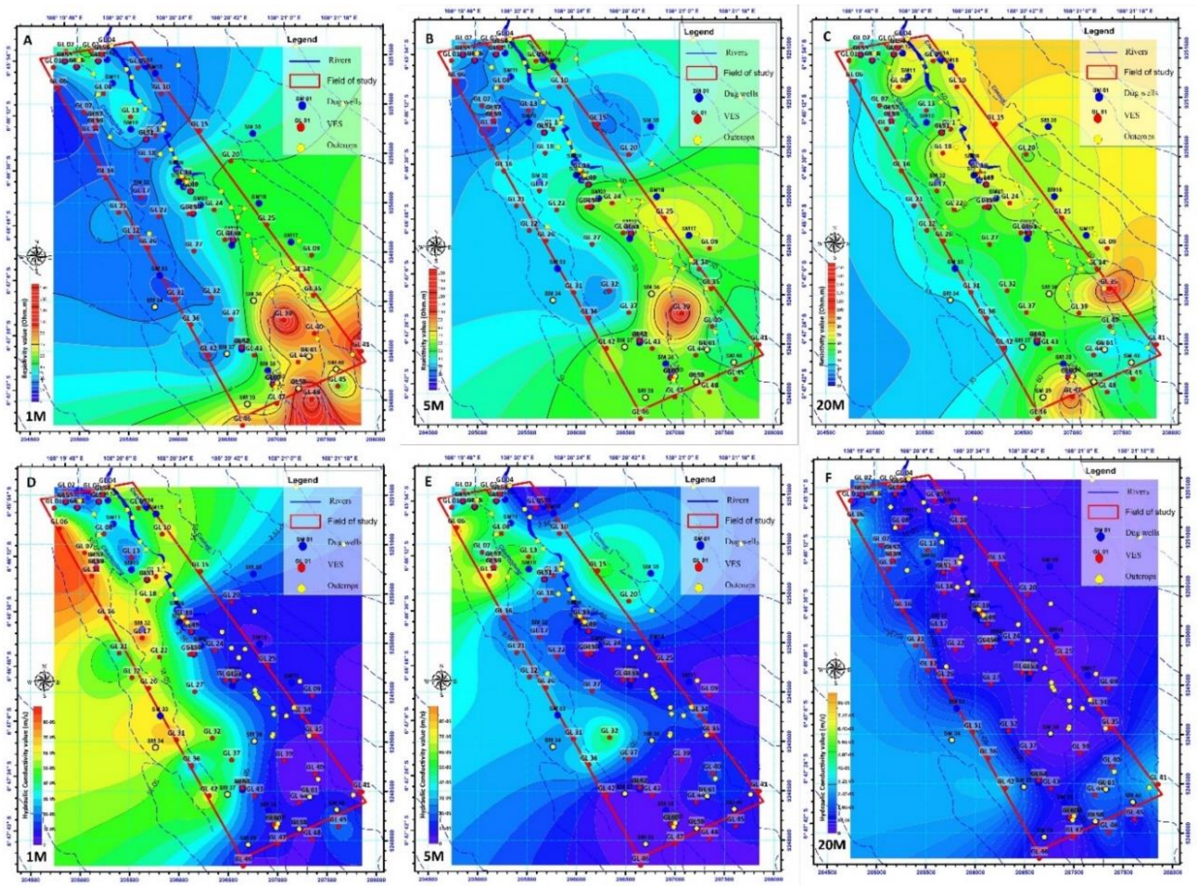

Figure 11. Contour map of (a) iso resistivity depth 1 m; (b) iso resistivity depth 5 m; (c) iso resistivity depth 20 m; (d) hydraulic conductivity computed by geoelectrical method depth 1 m; (e) hydraulic conductivity computed by geoelectrical method depth 5 m; (f) hydraulic conductivity computed by geoelectrical method depth 20 m.

geological map, the resistivity map at a depth of 1M and 5M shows the same pattern as the geological map of the study area. This shows that the rock properties affect the resistivity value (Hasan et al., 2018). Then, Figure 11c shows the resistivity map to a depth of 20 m with a resistivity value range of 42- 80 ohm.m. The resistivity pattern shown is relatively homogeneous in the study area. Then Figures 11 d, e, and f, show the estimated hydraulic conductivity maps at depths of 1m, 5m, and 20m with a value range of 4.97×10^{-6} to 6.75×10^{-5} m/s.

The value of hydraulic conductivity in the study area shows the aquifer potential in the low-high zone (Table 2). The high potential aquifer zone was estimated by $K > 4.62 \times 10^{-5}$ m/s. The medium potential aquifer zone was measured by K from 3.47×10^{-5} to 4.62×10^{-5} m/s. The low aquifer potential zone was revealed by $K <3.47\times 10^{-5}$ m/s (Hasan et al., 2021). Based on the correlation between resistivity and hydraulic conductivity in volcanic deposits shows an inverse correlation. Based on the theory of Ohm's law and Darcy's law, the inverse correlation between resistivity and hydraulic conductivity is due to the current flow in the horizontal direction being greater than the large vertical current flow (Niwas and De Lima, 2003). Based on the geological conditions on the north slope of Ciremai Volcano, the hydraulic conductivity value in the tuff breccia-pyroclastic breccia facies is lower than the lapilli tuff facies. This is because the breccia facies has poor sorting characteristics and is compact, so the fluid is difficult to flow.

Table 2. The delineated aquifer potential zones using different ranges of hydraulic conductivity

Aquifer potential	Hydraulic conductivity (m/s)
High potential aquifer	$> 4.62 \times 10^{-5}$
Medium potential aquifer	3.47×10^{-5} to 4.62×10^{-5}
Low potential aquifer	$<3.47\times 10^{-5}$

(Adapted from Hasan et al., 2021)

The aquifer parameters were calculated using geoelectrical methods by making proper proportions between the electrical and hydraulic parameters. However, such relations are established based on the local hydrogeological settings of the specific area and may not apply to other areas (Hasan et al., 2021). In this study, Kozeny's 1953 equation was chosen as it has been previously widely applied in porous aquifers (Kazakis et al., 2016; Soupios et al., 2007). The results of this research indicate that this equation successfully estimated the hydraulic conductivity of the studied aquifer.

4. CONCLUSIONS

Hydraulic conductivity is an important aquifer parameter in hydrogeological parameters. The above parameters are generally obtained by traditional methods such as pumping tests. However, this technique is expensive and difficult to perform in steep topographical areas. In addition, such a method cannot cover the entire area. Geophysical methods such as the sounding method are an alternative to traditional methods to improve hydraulic properties. However, the geoelectrical method alone cannot describe the aquifer parameters but can significantly reduce the number of wells. In this study, an innovative approach was carried out to determine the most appropriate parameter cementation factor (m) and alpha (α) for complex aquifer systems in volcanic deposits. This parameter is important for estimating the hydraulic parameters of aquifers using geoelectrical methods and petrophysical equations. On the northern slope of Mount Ciremai, geoelectrical methods can be used to determine porosity and hydraulic conductivity. The data obtained from the pumping test showed a strong correlation between these results. Finally, the resulting correlation of resistivity to hydraulic conductivity can be used in VES measurements that do not have wells for pumping tests.

5. ACKNOWLEDGMENTS

This study was a part of the thesis project research at the Faculty of Geology, Padjadjaran University, Indonesia. The authors like to thank the geophysics laboratory FTG UNPAD for assisting in the fieldwork and data analysis.

6. REFERENCES

Alfadli, M. K., & Natasia, N. (2017). Geoelectricity Data Analysis For Identification The Aquifer Configuration In Bandorasawetan, Cilimus, Kuningan, West Java Province. *Journal of Geoscience, Engineering, Environment, and Technology*, *2*(4), 278. doi: 10.24273/jgeet.2017.2.4.779

Amiri, V., Sohrabi, N., Li, P., & Shukla, S. (2022). Estimation of hydraulic conductivity and porosity of a heterogeneous porous aquifer by combining transition probability geostatistical simulation, geophysical survey, and pumping test data. *Environment, Development and Sustainability*. doi: 10.1007/s10668-022-02368-6

Archie, G. E. (1942). The Electrical Resistivity Log as an Aid in Determining Some Reservoir Characteristics. Transactions of the AIME, 146(01), 54–62. doi: 10.2118/942054-G

Archie, G.E. (1950). Introduction to Petrophysics of Reservoir Rocks. *AAPG Bulletin*, *34*. doi: 10.1306/3D933F62-16B1-11D7-8645000102C1865D

Cooper, H. H., & Jacob, C. E. (1946). A generalized graphical method for evaluating formation constants and summarizing well-field history. *Transactions, American Geophysical Union*, *27*(4), 526. doi: 10.1029/TR027i004p00526

Darisma, D., Fernanda, F., & Syukri, M. (2020). Investigation of Groundwater Potential using Electrical Resistivity Method and Hydraulic Parameters in Lam Apeng, Aceh Besar, Indonesia. *Journal of Geoscience, Engineering, Environment, and Technology*, *5*(4), 211–218. doi: 10.25299/jgeet.2020.5.4.5501

Djuri. (1995). Peta Geologi Lembar Arjawinangun, Jawa Barat. Direktorat Geol. dan Pengemb. Geol. Dep. Pertamb. dan Energi Republik Indonesia.

Domenico, P. A., & Schwartz, F. W. (1998). *Physical and chemical hydrogeology* (2nd ed). New York: Wiley.

Ezema, O. K., Ibuot, J. C., & Obiora, D. N. (2020). Geophysical investigation of aquifer repositories in Ibagwa Aka, Enugu State, Nigeria, using electrical resistivity method. *Groundwater for Sustainable Development*, *11*, 100458. doi: 10.1016/j.gsd.2020.100458

Fetter, C. W. (1994). Applied Hydrogeology: MacMillan College Publishing Co. *New York, NY,* 691p.

Gao, Q., Shang, Y., Hasan, M., Jin, W., & Yang, P. (2018). Evaluation of a Weathered Rock Aquifer Using ERT Method in South Guangdong, China. *Water*, *10*(3), 293. doi: 10.3390/w10030293

Hasan, M., Shang, Y., Akhter, G., & Jin, W. (2018). Geophysical Assessment of Groundwater Potential: A Case Study from Mian Channu Area, Pakistan. *Groundwater*, *56*(5), 783–796. doi: 10.1111/gwat.12617

Hasan, M., Shang, Y., Jin, W., & Akhter, G. (2021). Estimation of hydraulic parameters in a hard rock aquifer using integrated surface geoelectrical method and pumping test data in southeast Guangdong, China. *Geosciences Journal*, *25*(2), 223–242. doi: 10.1007/s12303-020-0018-7

Irawan, D. E., Puradimaja, D. J., Notosiswoyo, S., & Soemintadiredja, P. (2009). Hydrogeochemistry of volcanic hydrogeology based on cluster analysis of Mount Ciremai, West Java, Indonesia. *Journal of Hydrology*, *376*(1–2), 221–234. doi: 10.1016/j.jhydrol.2009.07.033

Ismawan, Rahayudin, Y., CSSA, B.Y., Suganda, B.R., Barkah, N. (2013). Airtanah Pada Endapan Volkanik Di Lereng Tenggara.

IWACO – WASECO. (1989). Kuningan Regency Provincial Water Supply Report.

Kazakis, N., Vargemezis, G., & Voudouris, K. S. (2016). Estimation of hydraulic parameters in a complex porous aquifer system using geoelectrical methods. *Science of The Total Environment*, *550*, 742–750. doi: 10.1016/j.scitotenv.2016.01.133

Kozeny, J. (Ed.). (1953). *Hydraulik*. Vienna: Springer Vienna. doi: 10.1007/978-3-7091-7592-7

Kwader, T. (1985). Estimating Aquifer Permeability from Formation Resistivity Factors.pdf. https://doi.org/10.1111/j.1745-6584.1985.tb01955.x

MacCary, L. M. (1978). Interpretation Of Well Logs In A Carbonate Aquifer. U.S. Geological Survey Open File Report 78-88, 30p.

Niwas, S., De Lima, O.A.L. (2003). Aquifer parameter estimation from surface resistivity data. Ground Water. https://doi.org/10.1111/j.1745-6584.2003.tb02572.x

Sattar, G. S., Keramat, M., & Shahid, S. (2016). Deciphering transmissivity and hydraulic conductivity of the aquifer by vertical electrical sounding (VES) experiments in Northwest Bangladesh. *Applied Water Science*, *6*(1), 35–45. doi: 10.1007/s13201-014-0203-9

Soupios, P. M., Kouli, M., Vallianatos, F., Vafidis, A., & Stavroulakis, G. (2007). Estimation of aquifer hydraulic parameters from surficial geophysical methods: A case study of Keritis Basin in Chania (Crete – Greece). *Journal of Hydrology*, *338*(1–2), 122–131. doi: 10.1016/j.jhydrol.2007.02.028

Telford, W.M., Geldart, L.P., Sheriff, R.E. (1990). Applied Geophysics, Second Edition. Cambridge Univ. Press.

Theis, C. V. (1935). The relation between the lowering of the Piezometric surface and the rate and duration of discharge of a well using ground-water storage. *Transactions, American Geophysical Union*, *16*(2), 519. doi: 10.1029/TR016i002p00519

Tizro, A. T., Voudouris, K. S., Salehzade, M., & Mashayekhi, H. (2010). Hydrogeological framework and estimation of aquifer hydraulic parameters using geoelectrical data: A case study from West Iran. *Hydrogeology Journal*, *18*(4), 917–929. doi:10.1007/s10040-010-0580-6

Ungemach, P., Mostaghimi, F., & Duprat, A. (1969). Essais de détermination du coefficient d'emmagasinement en nappe libre application a la nappe alluviale du rhin. *International Association Of Scientific Hydrology. Bulletin*, *14*(2), 169–190. Doi: 10.1080/02626666909493726

Winsauer, W. O., Shearin Jr, H. M., Masson, P. H., & Williams, M. (1952). Resistivity of brine-saturated sands in relation to pore geometry. *AAPG bulletin, 36*(2), 253-277. doi: 10.1306/3D9343F4-16B1-11D7-8645000102C1865D